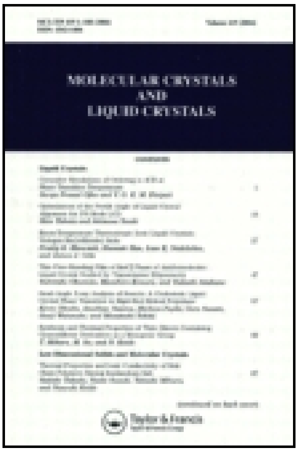

Molecular Crystals and Liquid Crystals
Publication details, including instructions for authors and subscription information:
http://www.tandfonline.com/loi/gmcl20

# Diphenylaminoarene/Chromene-containing Red Fluorescent Emitters for Organic Light-Emitting Diodes

Kum Hee Lee [a], Min Hye Park [a], Bo Min Seo [b], Ji Hoon Seo [b], Young Kwan Kim [b] & Seung Soo Yoon [a]

[a] Department of Chemistry, Sungkyunkwan University, Suwon, 440-746, Korea

[b] Department of Information Display, Hongik University, Seoul, 121-791, Korea

Version of record first published: 18 Oct 2011

To cite this article: Kum Hee Lee, Min Hye Park, Bo Min Seo, Ji Hoon Seo, Young Kwan Kim & Seung Soo Yoon (2011): Diphenylaminoarene/Chromene-containing Red Fluorescent Emitters for Organic Light-Emitting Diodes, Molecular Crystals and Liquid Crystals, 550:1, 260-269

To link to this article: http://dx.doi.org/10.1080/15421406.2011.599773

*Mol. Cryst. Liq. Cryst.*, Vol. 550: pp. 260–269, 2011

ISSN: 1542-1406 print/1563-5287 online
DOI: 10.1080/15421406.2011.599773

Taylor & Francis
Taylor & Francis Group

# Diphenylaminoarene/Chromene-containing Red Fluorescent Emitters for Organic Light-Emitting Diodes

KUM HEE LEE,[1] MIN HYE PARK,[1] BO MIN SEO,[2]
JI HOON SEO,[2] YOUNG KWAN KIM,[2,*]
AND SEUNG SOO YOON[1,*]

[1]Department of Chemistry, Sungkyunkwan University, Suwon, 440-746, Korea
[2]Department of Information Display, Hongik University, Seoul, 121-791, Korea

*In this study, we synthesized new 2-(2-(4-(diphenylamino)styryl)-4*H*-chromen-4-ylidene) malononitrile (DCCPA) derivatives with different $\pi$-conjugation aromatic spacer groups between the diphenylamine and (chromen-4-ylidene)malononitrile moieties of the DCCPA. To explore the electroluminescence properties of these materials, multilayered OLEDs were fabricated with a device stricture of: Indium Tin Oxide (ITO) (170 nm)/*N,N'*-diphenyl-*N,N'*-(1-napthyl)-(1,1'-phenyl)-4,4'-diamine (NPB) (50 nm)/2-methyl-9,10-bis-2-naphthyl anthracene (MADN):Red dopants **1** (5, 10%) (30 nm)/bis-(2-methyl-8-quinolinolato-$N_1$,$O_8$)-(1,1'-biphenyl-4-olato)aluminum (Balq) (30 nm)/Liq (2 nm)/Al (10 nm). A device using **Red 1** showed a maximum luminance of 1030 cd/m$^2$ at 10.0 V, with maximum luminous, power, and quantum efficiencies of 0.94 cd/A, 0.54 lm/W, and 1.11%, respectively. The CIE coordinates of this device were (0.61, 0.35) at 7.0 V, a stable color chromaticity at various voltages.*

**Keywords** OLED; Red fluorescent emitter; Chromene derivatives.

## Introduction

Organic light-emitting diodes (OLEDs) have attracted a great deal of attention due to their potential uses in full color flat-panel displays and solid-state lighting [1]. Compared to blue and green fluorescent emitting materials, red OLEDs have inferior EL performances [2, 3]. Thus, there has been much research in the development of highly efficient red fluorescent emitting materials [4, 5]. However, development of new red fluorescent emitters with excellent electroluminescence properties is not without difficulty as their luminescence quantum yields tend to decrease with increasing emission peak wavelength according to the energy gap law [6].

Recently, Lee *et al*. reported a red fluorescent OLED, using the red fluorescence material 2-(2-(4-(diphenylamino)styryl)-4H-chromen-4-ylidene)malononitrile (DCCPA) as a dopant, that exhibited a power efficiency of 0.14 lm/W and Commission Internationale

---

*Corresponding author. E-mail: kimyk@hongik.ac.kr (Y. K. Kim); ssyoon@skku.edu (S. S. Yoon)

de L'Eclairage (CIE) coordinates of (0.60, 0.39). However, its EL efficiencies require improvement for practical application. Furthermore, this device presents far-from-ideal CIE coordinates for the saturated red color, which is close to (0.67, 0.33) [7, 8].

In this study, this lab synthesized new DCCPA derivatives with different $\pi$-conjugation aromatic spacer groups between the diphenylamine and (chromen-4-ylidene)malononitrile moieties of DCCPA to improve the color purity of OLEDs using DCCPA. Three different spacer groups (naphthalene, biphenyl, 9,9,-diethyl fluorine) were incorporated to control $\pi$-conjugation length of the fluorophore and thus, color chromaticity of OLED devices using it. Furthermore, the different spacer groups change the various physical properties of the emitting materials, including HOMO/LUMO energy levels, quantum yields, and degree of energy transfer, leading to improved EL performance of the OLEDs using them. As will be described below, an OLED using 2-(2-(2-(6-(diphenylamino)naphthalen-2-yl)vinyl)-4H-chromen-4-ylidene)malononitrile as a dopant exhibited efficient red emissions with improved EL performances in comparison to DCCPA-based OLED devices.

## Experimental

### *Materials and Measurements*

All $^1$H- and $^{13}$C-NMR spectra were recorded on a Varian (300 or Unity Inova 300Nb or Unity Inova 500Nb) spectrometer. All FT-IR spectra were recorded using a Bruker VERTEX70 FT-IR spectra spectrometer. Low- and high-resolution mass spectra were measured using a Varian 500-MS spectrometer in the fast atom bombardment (FAB) mode, a JEOL JMS-600W spectrometer in the electron ionization (EI) mode, and a JMS-T100TD (AccuTOF-TLC) spectrometer in the positive-ion mode. The ultraviolet-visible (UV-Vis) absorption and photoluminescence (PL) spectra of the newly designed red dopants were measured in $10^{-5}$ M $CH_2Cl_2$. The fluorescent quantum yield was determined in $CH_2Cl_2$ at 293 K against DCCPA ($\Phi = 0.54$) [9]. The highest occupied molecular orbital (HOMO) energy level was measured by low-energy photoelectron spectrometry (Riken Keiki AC-2). The lowest unoccupied molecular orbital (LUMO) energy level was estimated by subtracting the energy gap from the HOMO energy level.

2-(2-(2-(6-(diphenylamino)naphthalen-2-yl)vinyl)-4H-chromen-4-ylidene) malononitrile (**Red 1**). Compound 6-(diphenylamino)-2-naphthaldehyde (1.83 mmol) and propanedinitrile, 2-(2-methyl-4H-1-benzopyran-4-ylidene) (1.83 mmol) were placed into an RBF connected to a Dean-Stark trap (with a molecular sieve) and a reflux condenser. Then, anhydrous ethyl alcohol (15 mL) and piperidine (8.23 mmol) were added and refluxed from 90 to 100 °C for 12 h, followed by cooling to room temperature. The mixture was then filtered and purified by re-crystallization from $CH_2Cl_2$ and hexane. The obtained compound was a reddish solid. (Yield: 52%). $^1$H-NMR (300 MHz, $CDCl_3$): $\delta$ (ppm) 8.93 (dd, $J = 1.3$, 8.4 Hz, 1H), 7.89 (s, 1H), 7.79–7.71 (m, 3H), 7.63–7.56 (m, 3H), 7.46 (t, $J = 6.1$ Hz, 1H), 7.34–7.28 (m, 6H), 7.18–7.13 (m, 4H), 7.12–7.09 (m, 2H), 6.90–6.85 (m, 2H); $^{13}$C-NMR (125 MHz): $\delta$ (ppm) 158.2, 153.0, 152.6, 151.0, 148.5, 148.0, 144.6, 140.0, 135.4, 134.8, 132.8, 129.5, 128.2, 126.1, 124.5, 123.4, 122.2, 121.3, 119.8, 118.8, 117.4, 116.1, 106.8, 56.4; FT-IR (KBr): $\nu = 2205$, 1494, 1481, 1195, 700 (cm$^{-1}$); Mass (EI – MS) $m/z = 514$ ($M^+$+H); HRMS calcd for $C_{36}H_{23}N_3O$, 513.1841; found, 513.1845; mp: 295 °C.

2-(2-(2-(4'-(diphenylamino)biphenyl-4-yl)vinyl)-4H-chromen-4-ylidene) malononitrile (**Red 2**). Compound **Red 2** was prepared by method of **Red 1** using

6-(diphenylamino)-2-naphthaldehyde instead of 4'-(diphenylamino)biphenyl-4-carbaldehyde. The obtained compound was reddish solid (Yield : 45%). $^1$H-NMR (300 MHz, $CDCl_3$): $\delta$ (ppm); 8.93 (dd, $J = 1.2, 7.2$ Hz, 1H), 7.77–7.64 (m, 3H), 7.59–7.53 (m, 4H), 7.45 (t, $J = 7.7$ Hz, 1H), 7.30–7.25 (m, 4H), 7.14–7.10 (m, 5H), 7.06–7.02 (m, 3H), 6.89–6.83 (m, 2H), 2.05–2.00 (m, 4H), 0.39 (t, $J = 7.2$ Hz, 6H); $^{13}$C-NMR (125 MHz): $\delta$ (ppm) 158.2, 153.0, 152.6, 151.0, 148.5, 148.0, 144.6, 140.0, 135.4, 134.8, 132.8, 129.5, 128.2, 126.1, 124.5, 123.4, 122.2, 121.3, 119.8, 118.8, 117.4, 116.1, 106.8, 56.4; FT-IR (KBr): $\nu = 2208, 1628, 1592, 1556, 1481, 1464, 1454, 1201, 815$ cm$^{-1}$; Mass (EI – MS) $m/z = 540$ ($M^+$+H); HRMS calcd for $C_{38}H_{25}N_3O$, 539.1998; found, 539.1992; mp: 249°C.

2-(2-(2-(7-(diphenylamino)-9,9-diethyl-9H-fluoren-2-yl)vinyl)-4H-chromen-4-ylidene)malononitrile (**Red 3**). Compound **Red 3** was prepared by method of DCCPA using 6-(diphenylamino)-2-naphthaldehyde instead of 7-(diphenylamino)-9,9-diethyl-9H-fluorene-2-carbaldehyde. The obtained compound was reddish solid (Yield : 84%). $^1$H NMR (300 MHz, $CDCl_3$): 8.91 (dd, $J = 1.2, 8.4$ Hz, 1H), 7.75 (t, $J = 7.2$ Hz, 1H), 7.68–7.62 (m, 5H), 7.57 (d, $J = 7.5$ Hz, 1H), 7.51 (d, $J = 8.7$ Hz, 2H), 7.45 (t, $J = 8.4$ Hz, 1H), 7.31–7.26 (m, 5H), 7.16–7.13 (m, 6H), 7.06 (t, $J = 7.3$ Hz, 2H), 6.88–6.79 (m, 2H), $^{13}$C-NMR (125 MHz, $CDCl_3$) : 157.8, 153.0, 152.6, 148.2, 147.7, 143.0, 138.8, 134.9, 133.4, 129.6, 128.8, 127.9, 127.3, 126.2, 125.0, 123.6, 118.8, 118.3, 118.1, 117.0, 116.0, 107.1, 62.9, FT-IR (ATR): v (cm-1) : 2205, 1494, 1481, 1195, 700; FT-IR (KBr): $\nu = 2205, 1494, 1481, 1195, 700$ cm$^{-1}$; Mass (EI – MS) $m/z = 608$ ($M^+$+H); HRMS calcd for $C_{43}H_{33}N_3O$, 607.2624; found, 607.2629; mp: 276°C.

## Results and Discussion

The synthesis of **Red 1 - 3** is shown in Scheme 1. Knoevenagel condensation of the corresponding aldehyde intermediates[10–12] with 2-(2-methyl-4H-1-benzopyran-4-ylidene)malononitrile provided red emitters **1 - 3** in moderate yield. These compounds were fully characterized with $^1$H- and $^{13}$C-NMR, infrared (IR), and low- and high-resolution mass spectrometry.

The UV-Vis absorption and PL spectra of **DCCPA** and **Red 1 - 3** are shown in Fig. 1. The maximum absorption peaks of **DCCPA** and **Red 1 - 3** were observed at 452, 493, 494, and 494 nm, respectively. The absorption of each compound showed good spectral overlap with the emissions of the MADN in the host, indicating that MADN serves as a suitable host in the OLEDs using **DCCPA** and **Red 1 - 3** as red dopant materials. In the PL spectra, the maximum emission wavelengths ($\lambda_{max}$) of **DCCPA** and **Red 1 - 3** appeared at 646, 681, 640, and 703 nm in the proper red region of the visible spectrum, respectively. Interestingly, compared to **DCCPA**, the maximum emission peaks of **Red 1** and **3** in the solution state were red-shifted by 35 and 55 nm, respectively, due to the extended $\pi$-conjugation length of **Red 1** and **3** by the naphthalene and 9,9'-diethylfluorene spacer groups. The PL quantum yields of **Red 1 - 3** were found to be 0.31, 0.15, and 0.08, respectively, using **DCCPA** as the standard. The HOMO level was measured with a photoelectron spectrometer used in a Riken Keiki AC-2, and the LUMO level computed using the optical band gap energy and HOMO level. The HOMO and LUMO energy levels of **Red 1 - 3** were -5.36 to -5.49 eV and -3.20 to -3.44 eV, respectively. All physical data are summarized in Table 1.

Among red emitters **1 - 3**, **Red 1** has the proper maximum emission peak and quantum yield in the solution state for the red-emitting material. Thus, its electroluminescent properties were explored by fabrication of a device using **Red 1** as the dopant. The device structure with the HOMO and LUMO energy levels of the materials used in the devices are

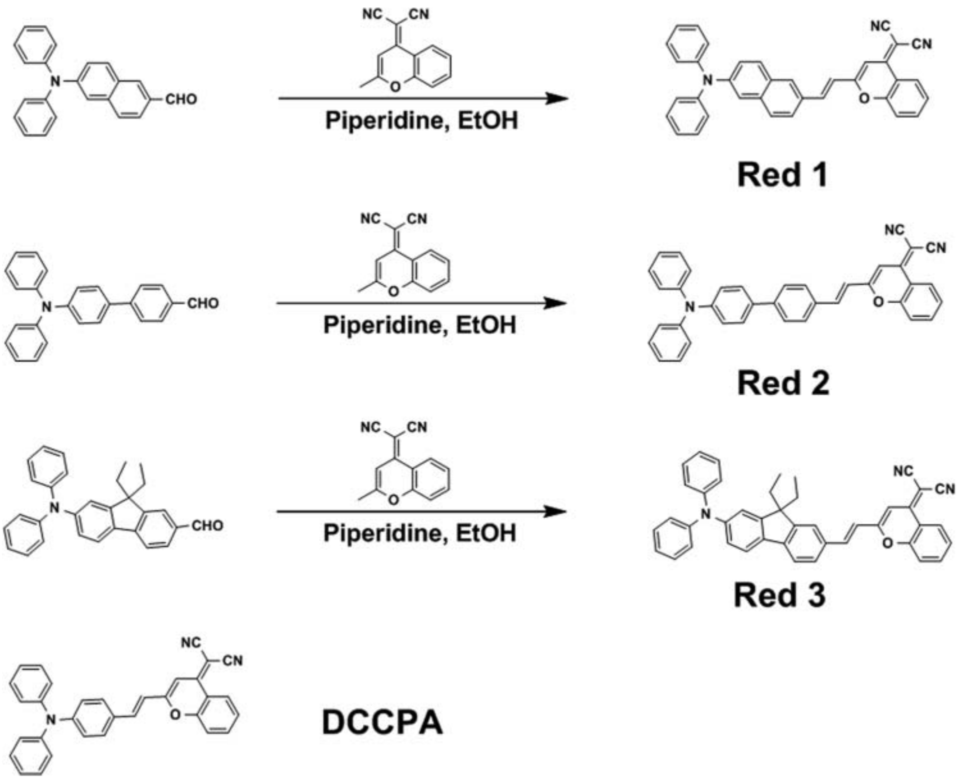

**Scheme 1.** Synthesis and structures of red emitters (**Red 1–3**, and DCCPA).

shown in Fig. 2. The NPB was introduced as a hole-transporting layer (HTL) to enhance hole-injection and transport, while Balq and Liq were introduced as an electron-transporting layer (ETL) and electron-injecting layer (EIL) to enhance electron-injection and transport. The emitting layers of these devices were composed of MADN host and **Red 1** or **DCCPA** as dopants. All electroluminescent data is summarized in Table 2.

The (a) current density-voltage (*J*-*V*) and (b) luminance-voltage (*L*-*V*) characteristics of devices **1** - **3** are shown in Fig 3. The maximum current densities of devices **1** - **3** were

**Table 1.** Physical properties of red dopants **DCCPA** and **Red 1** - **3**

| Compound | $UV_{max}$ (nm)[a] | $PL_{max}$ (nm)[b] | FWHM | HOMO (eV)[b] | LUMO (eV)[b] | $E_g$ | Q.Y[c] | mp(°C) |
|---|---|---|---|---|---|---|---|---|
| DCCPA | 452 | 646 | 110 | −5.40 | −3.25 | 2.15 | 0.54 | - |
| Red 1 | 493 | 681 | 119 | −5.36 | −3.27 | 2.09 | 0.31 | 295 |
| Red 2 | 494 | 640 | 95 | −5.42 | −3.20 | 2.22 | 0.15 | 249 |
| Red 3 | 494 | 703 | 100 | −5.49 | −3.44 | 2.05 | 0.08 | 276 |

[a, b] Maximum absorption or emission wavelength in $CH_2Cl_2$ (ca. $1 \times 10^{-5}$M) [b] Obtained from AC-2 and UV-vis absorption measurements. [c] Using DCCPA as a standard; $\lambda_{ex} = 550$ nm ($\Phi = 0.54$ in $CH_2Cl_2$).

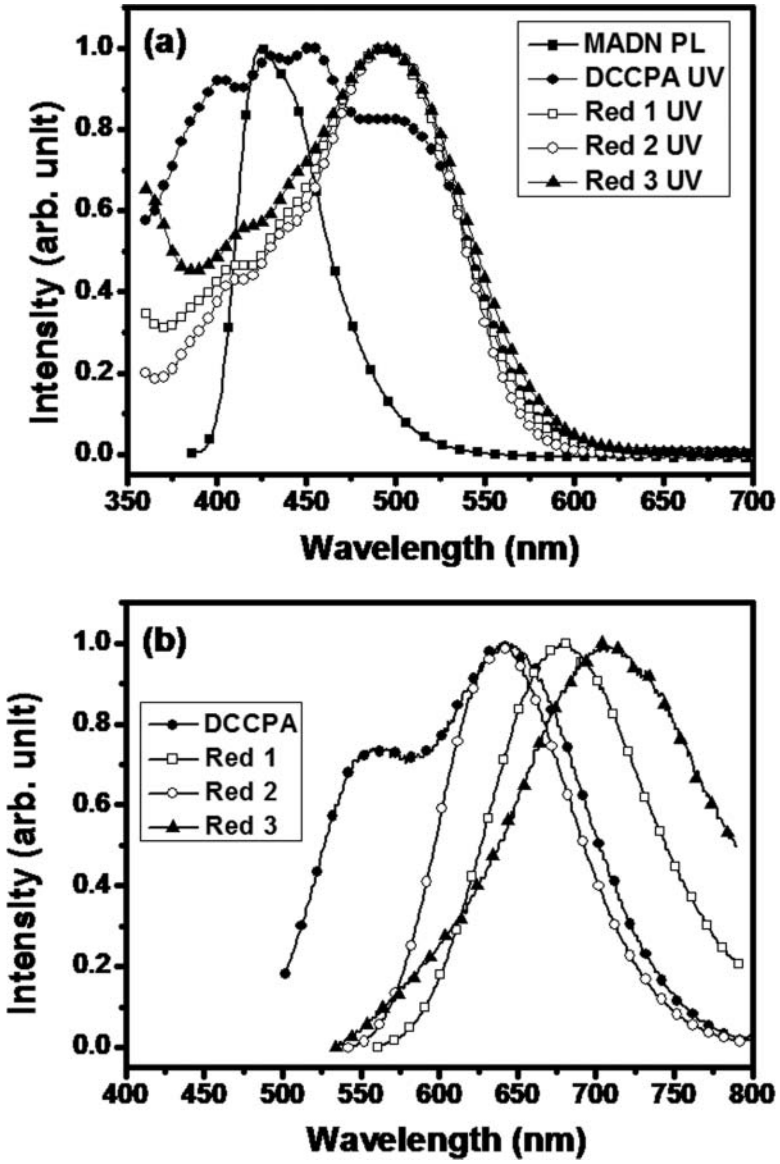

**Figure 1.** (a) UV-Vis absorption spectra and (b) Photoluminescence spectra of red dopants **DCCPA** and **Red 1** - **Red 3**.

176, 128, and 115 mA/cm$^2$, and the maximum luminances devices were 883, 1030, and 808 cd/m$^2$ at 12.0 V, respectively. Additionally, the turn-on voltages were 5.0, 4.5, and 4.5 V, respectively. Compared to device **1** using **DCCPA**, device **2** using **Red 1** at the same doping concentration showed an improved luminance and turn-on voltage.

The luminous, power, and quantum efficiencies of devices **1 - 3** are shown in Fig. 4. Their respective luminous efficiencies were 0.66, 0.87, and 0.75 cd/A at 20 mA/cm$^2$, while their power efficiencies were 0.28, 0.36, and 0.31 lm/W at 20 mA/cm$^2$, respectively. Furthermore, the external quantum efficiencies of devices **1 - 3** were 0.39, 0.95, and

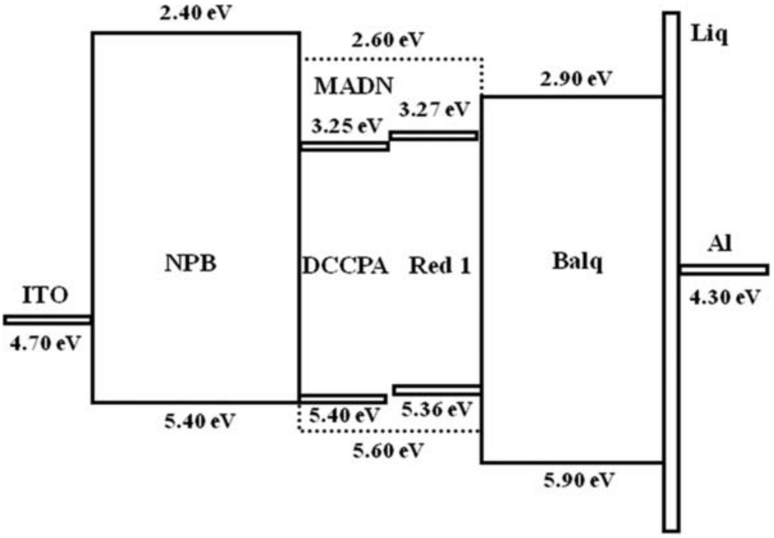

**Figure 2.** Energy-level diagram of OLEDs.

0.15% at 20 mA/cm$^2$, respectively. Compared to device **1** using **DCCPA** at a 5% doping concentration, device **2** using **Red 1** at the same doping concentration had improved EL efficiencies. For example, the luminous, power and external quantum efficiencies of device **2** were increased by 32, 29, and 171% at 20 mA/cm$^2$, respectively, in comparison to those of device **1**. The HOMO energy level of **Red 1**, as a dopant in device **2**, was higher by 0.04 eV than that of **DCCPA** as a dopant in device **1**. This lead the more effective direct-hole trapping into the dopant in device **2** than device **1**, and thus, the improved EL efficiencies of device **2** in comparison to **1**. However, the possibilities that other factors such as the effective exciton formation and carrier balance in device **2** could contributed to the improved EL efficiencies of device **2**, in comparison to device **1**, cannot be excluded. In devices **2** and **3** using **Red 1** as a dopant at different doping concentrations, the increase in doping concentration reduced EL efficiencies. For example, the increase in doping concentration of **Red 1** from 5 to 10% reduced both luminous and power efficiencies by 14% at 20 mA/cm$^2$, respectively. Presumably, the concentration quenching at high doping concentration of **Red 1** would lead the reduced EL efficiencies of device **3**.

**Table 2.** EL performance characteristic of device**s** **1** and **2**

| Device [Dopant (%)] | L[a] (cd/m$^2$) | LE[b]/[c] (cd/A) | PE[b]/[c] (lm/W) | QE[b]/[c] (%) | EL[d] (nm) | CIE[d] (x,y) |
|---|---|---|---|---|---|---|
| 1 [DCCPA (5%)] | 883 | 0.66/0.74 | 0.28/0.39 | 0.39/0.45 | 610 | (0.54, 0.40) |
| 2 [Red 1 (5%)] | 1030 | 0.87/0.94 | 0.36/0.54 | 0.95/1.11 | 639 | (0.61, 0.35) |
| 3 [Red 1 (10%)] | 808 | 0.75/0.85 | 0.31/0.48 | 1.15/1.38 | 654 | (0.62, 0.34) |

[a] Maximum luminance at 10.0 V, [b] Value measured at 20 mA/cm$^2$, [c] Maximum values, [d] Value measured at 7.0 V.

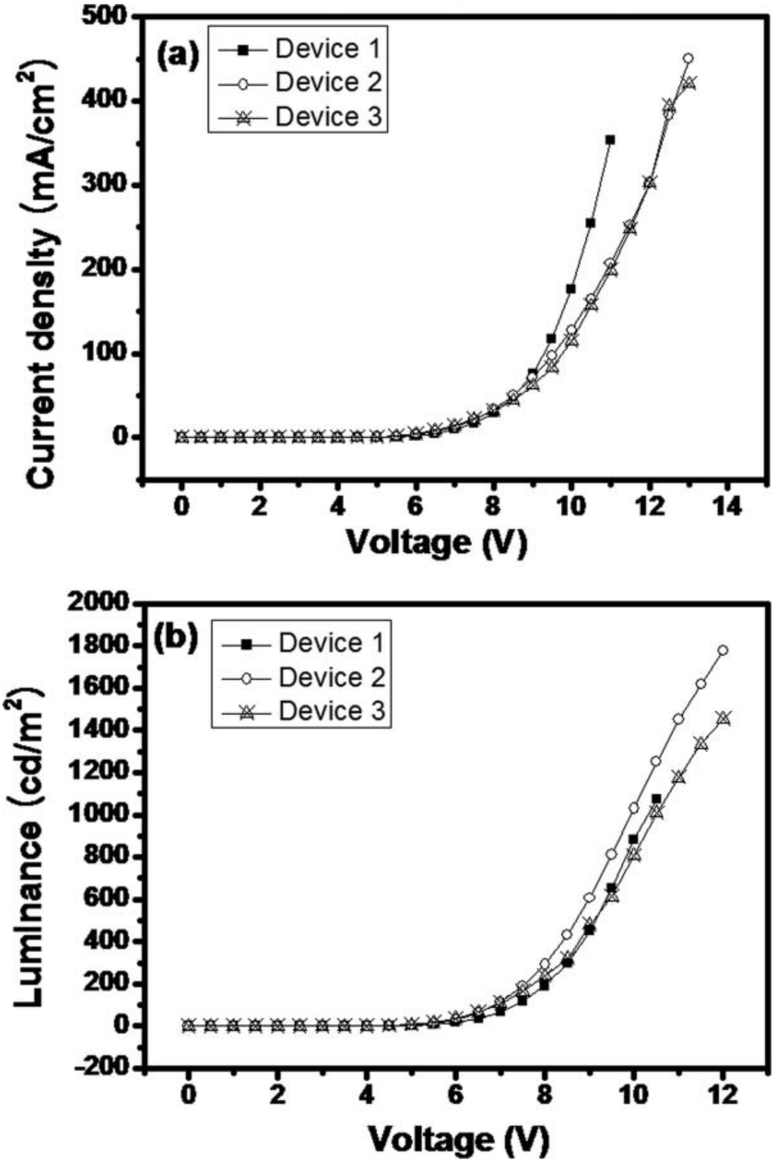

**Figure 3.** (a) Current density-Voltage and (b) Luminance-Voltage characteristics of the devices **1** - **3**.

The electroluminescent emission spectra and Commission International de L'Éclairage (CIE) coordinates of devices **1** - **3** are shown in Fig. 5. The maximum peaks in EL spectra of devices **1** - **3** were 610, 639, and 654 nm, respectively. Compared to device **1**, the maximum emission peak in the EL spectrum of device **2** was red-shifted by 29 nm due to the extended $\pi$-conjugation length of dopant **Red 1**. In devices **2** and **3** using **Red 1** as a dopant at different doping concentrations, the increase in doping concentration improved color chromaticity. For example, the increase in doping concentration of **Red 1** from 5 to 10% increased the maximum emission peaks in the EL spectra by 15 nm. Presumably, the

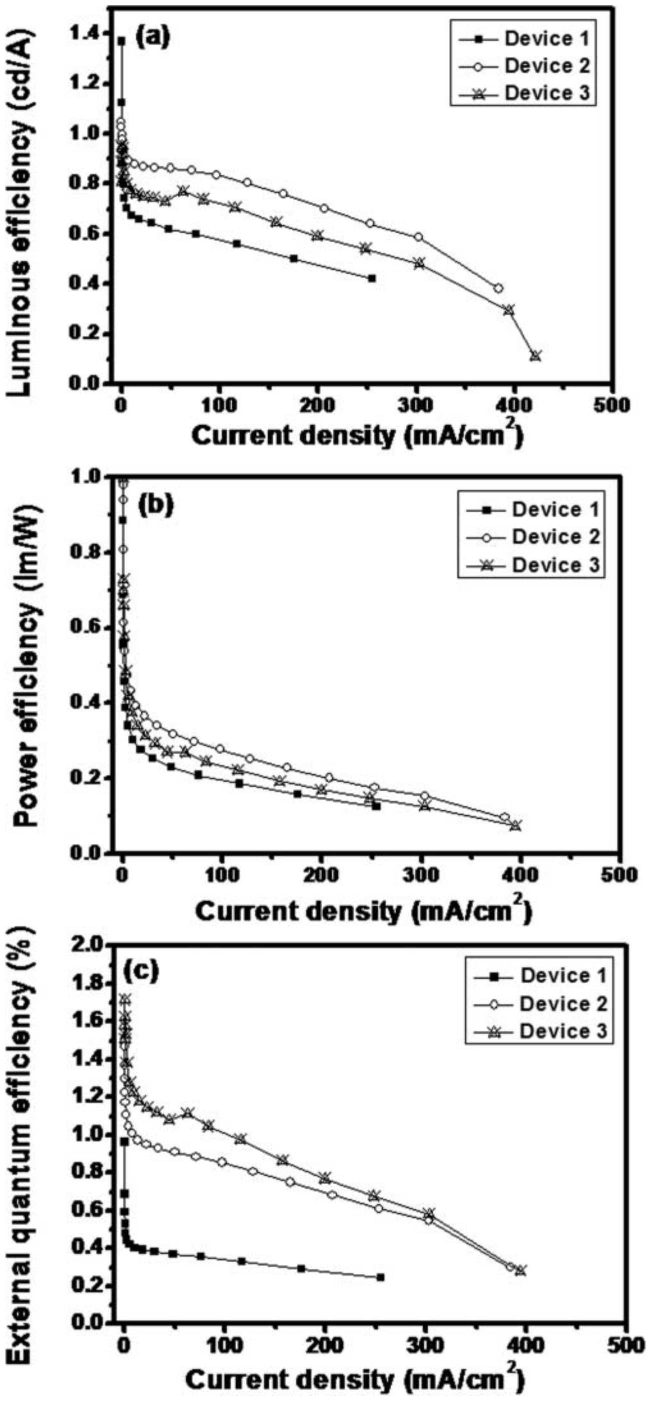

**Figure 4.** (a) Luminous efficiency, (b) Power efficiencies, and (c) external quantum efficiency-current density characteristics of devices **1** - **3**.

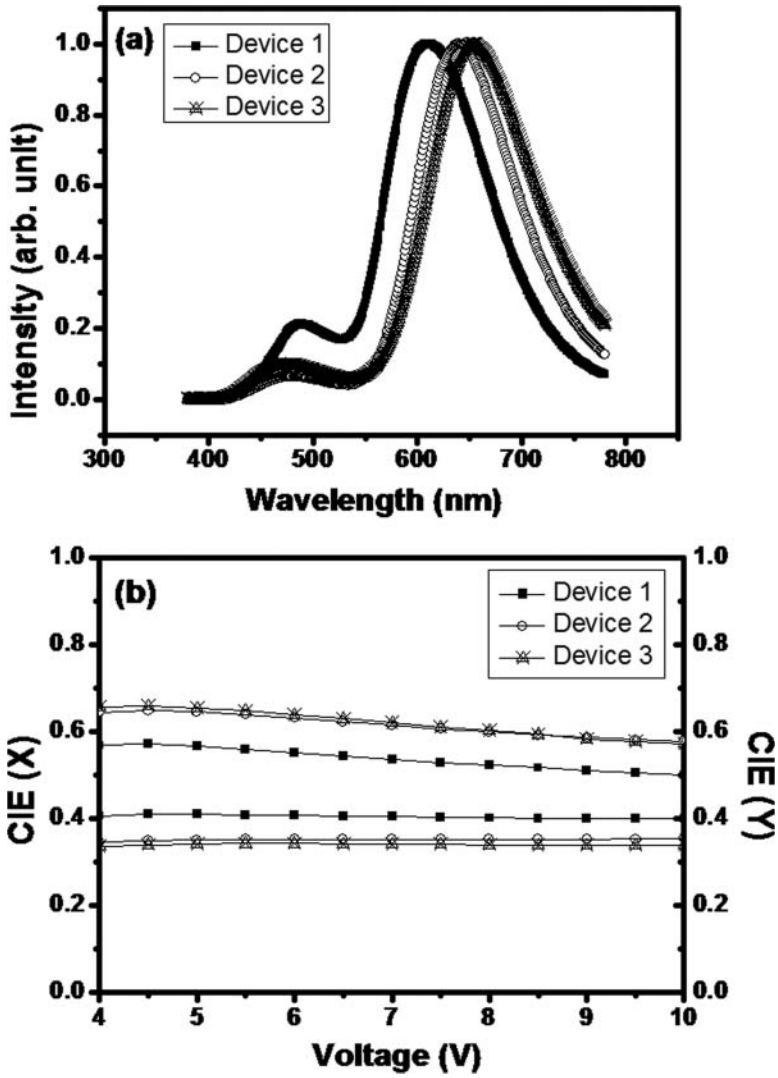

**Figure 5.** (a) EL spectra and (b) CIE coordinates of the devices **1** - **3**.

excimer formation at the high doping concentration of **Red 1** would lead to the red-shifted maximum emission peak in EL spectrum of device **3,** in comparison to device **2**. In the EL spectra of device **1** - **3**, there were shoulder peaks near 480 nm, possibly originating from the exciplex between the MADN host and NPB at the interface of the emitting and hole-transporting layers [13–16]. Interestingly, the shoulder peak of the EL spectrum of device **2** using **Red 1** is much smaller than that of device **1** using **DCCPA**. This observation implies that the exciton formation at **Red 1** dopant in device **2** is more effective than that of **DCCPA** in device **1**, due to the more effective hole-trapping in device **2** by the higher-lying HOMO energy level of **Red 1** than that of **DCCPA**. The values of the CIE coordinates of devices **1** - **3** were (0.54, 0.40), (0.61, 0.35), and (0.62, 0.34) at 7.0 V, respectively. Furthermore, devices **1** - **3** showed a stable color chromaticity with various voltages. Compared to device **1** using **DCCPA** as a dopant, device **2** has an improved color chromaticity.

## Conclusions

Efficient diphenylaminoarene/chromene-containing red fluorescent materials were newly designed and synthesized. An OLED device employing **Red 1,** with naphthalene spacer groups, as a dopant showed a maximum luminance of 1030 cd/m$^2$ at 10.0 V, along with maximum luminous, power, and quantum efficiencies of 0.94 cd/A, 0.54 lm/W, and 1.11%, respectively. The CIE coordinates of this device were (0.61, 0.35) at 7.0 V, a stable color chromaticity at various voltages.

## References

[1] Bulovic. A, Shoustikov. A, Baldo. M. A, Bose. E, and Kozlov. V. G., *Chem. Phys. Lett.*, **287**, 455 (1998).

[2] Li. J, Liu. D, Hong. Z, Tong. S, Wang. P, Ma. C, Lengyel. O, Lee. C. S, Kwong. H. L, and Lee. S., *Chem. Mater.*, **15** 1486 (2003).

[3] Tang. C. W, VanSlyke. S. A, and Chen. C. H., *J. Appl. Phys.*, **65**, 3610 (1989).

[4] Yao. Y. S., Zhou. Q. X., Wang. X. S., Wang. Y., and Zhang. B. W., *Adv. Funct. Mater.*, **17**, 93 (2007).

[5] Zhao. P., Tang. H., Zhang. Q., Pi. Y., Xu. M., Sun. R., and Zhu. W., *Dyes. Pigment.* **82**, 316 (2009).

[6] Divya. O. and Mishra. A. K., *Anal. Chim. Acta*, **630**, 47 (2008).

[7] Zhang. X. H, Chen. B. J, Lin. X. Q, Wong. O. Y, Lee. C. S, Kwong. H. L, Lee. S. T, and Wu. S. K., *Chem. Mater.*, **13**, 1565 (2001).

[8] Chen. J, Sun. X. W, Lin. X. Q, Lee. C. S, and Lee. S. T., *Mater Sci & Eng.*, **59**, B100 (2003).

[9] Ho. M. H, Wu. Y. S, Wen. S. W, Lee. M. T, Chen. T. M, Chen. C. H, Kwok. K. C, So. S. K, Yeung. K. T, Cheng. Y. K, and Gao. J. Q., *Appl. Phys. Lett.*, **89**, 252903 (2006).

[10] Chen. C, Li. Y. F, and Yang. L. M., *J. Mol. Cat. A.*, **269**, 158 (2007).

[11] Kowalski. K, Long. N. J, Kuimova. M. K, Kornyshev. A. A, Taylor. A. G, and White. A. J. P., *New J. Chem.*, **33**, 598 (2009).

[12] Baheti. A, Tyagi. P, Justin Thomas. K. R, Hsu. Y. C, and Lin. J. T., *J. Phys. Chem. C.*, **113**, 8541 (2009).

[13] Zhao. D, Zhang. F, Xu. C, Sun. J, Song. S, Xu. Z, and Sun. X., *Applied Surface Science.*, **254**, 3548 (2008).

[14] Palilis. L. C, Maminen. A. J, Uchida. M, and Kafafi. Z. H., *Appl. Phys. Lett.*, **82**, 2209 (2003).

[15] Matsumoto. N and Adachi. C., *J. Phys. Chem. C.*, **114**, 4652 (2010).

[16] Su. W. M, Li. W. L, Xin. Q, Su. Z. C, Chu. B, Bi. D. F, He. H, and Niu. J. H., *Appl. Phys. Lett.*, **91**, 043508 (2007).